JOURNAL OF AGRICULTURAL AND FOOD CHEMISTRY

J. Agric. Food Chem. **2004,** *52,* 2681−2688 **2681**

Dynamic High-Resolution ^{1}H and ^{31}P NMR Spectroscopy and ^{1}H T_2 Measurements in Postmortem Rabbit Muscles Using Slow Magic Angle Spinning

HANNE CHRISTINE BERTRAM,*,† JIAN ZHI HU,‡ DONALD N. ROMMEREIM,‡ ROBERT A. WIND,‡ AND HENRIK J. ANDERSEN†

Department of Food Science, Research Center Foulum, Danish Institute of Agricultural Sciences, P.O. Box 50, DK-8830 Tjele, Denmark, and Pacific Northwest National Laboratory, P.O. Box 999, MS K8-98, Richland, Washington 99352

Postmortem changes in rabbit muscle tissue with different glycogen status (normal vs low) were followed continuously from 13 min postmortem until 8 h postmortem and again 20 h postmortem using simultaneous magic angle spinning ^{1}H and ^{31}P NMR spectroscopy together with measurement of the transverse relaxation time, T_2, of the muscle water. The ^{1}H metabolite spectra were measured using the phase-altered spinning sidebands (PASS) technique at a spinning rate of 40 Hz. pH values calculated from the ^{31}P NMR spectra using the chemical shifts of the C-6 line of histidine in the ^{1}H spectra and the chemical shifts of inorganic phosphate in the ^{31}P spectra confirmed the different muscle glycogen status in the tissues. High-resolution ^{1}H spectra obtained from the PASS technique revealed the presence of a new resonance line at ∼6.8 ppm during the postmortem period, which were absent in muscles with low muscle glycogen content. This new resonance line may originate from the aminoprotons in creatine, and its appearance may be a result of a pH effect on the exchange rate between the amino and the water protons and thereby the NMR visibility. Alternatively, the new resonance line may originate from the aromatic protons in tyrosine, and its appearance may be a result of a pH-induced protein unfolding exposing hydrophobic amino acid residues to the aqueous environment. Further studies are needed to evaluate these hypotheses. Finally, distributed analysis of the water T_2 relaxation data revealed three relaxation populations and an increase in the population believed to reflect extramyofibrillar water through the postmortem period. This increase was significantly reduced ($p < 0.0001$) in samples from animals with low muscle glycogen content, indicating that the pH is controlling the extent of postmortem expulsion of water from myofibrillar structures. The significance of the postmortem increase in the amount extramyofibrillar water on the water-holding capacity was verified by centrifugation, which showed a reduced centrifugation loss in muscles with low preslaughter glycogen status (0.9 vs 1.9%, $p = 0.07$).

KEYWORDS: Muscle water; water-holding capacity; muscle metabolism; pH; adrenaline; MAS; creatine

INTRODUCTION

During the conversion of muscle to meat, several biochemical and biophysical processes are taking place that determine the meat quality (*1*). Energy-demanding muscle contractions continue to take place after death, resulting in a continued consumption of adenosine triphosphate (ATP) and phosphocreatine (PCr). In addition, lactate is formed as a consequence of glycogen degradation under anaerobic conditions and accumulated in the muscles with a resultant decrease in pH postmortem. Furthermore, the limitation in oxygen supply (anoxia) results in intracellular osmotic perturbation within muscle cells, which may trigger a redistribution of the water and thereby affect the final meat quality (*2*). Accordingly, the postmortem processes determining the meat quality are multifactorial and complex, and studying a single parameter will fail to provide a complete picture of the conversion of muscle to meat. Therefore, introducing methodologies that could combine measurement of various metabolites, pH, and water properties could have substantial significance for understanding the relationship between the biochemical and the biophysical processes and meat quality. NMR methodologies are very attractive as they allow noninvasive and continuous measurements of the ongoing processes within muscles.

Measurement of ^{1}H transverse relaxation time, T_2, of muscle water is proven to be a successful method in the determination of water-holding capacity (WHC) of pork (*3*−*7*), and a recent

* To whom correspondence should be addressed. Tel: +45 89 99 15 06. Fax: +45 89 99 15 64. E-mail: HanneC.Bertram@agrsci.dk.
† Danish Institute of Agricultural Sciences.
‡ Pacific Northwest National Laboratory.

10.1021/jf030614y CCC: $27.50
Published on Web 04/07/2004

study has shown that T_2 provides information about alterations in water compartmentalization and mobility during the conversion of muscle to meat that are decisive for the final WHC of the meat (*8*). In addition, the use of ^{31}P NMR spectroscopy to study phosphorus metabolites and pH in postmortem muscle tissue, which was initially demonstrated by Hoult et al. (*9*), has been applied extensively (*10*−*15*). In contrast, the use of proton NMR metabolite spectroscopy to study postmortem muscles is very limited (*16*). This is most probably due to the fact that proton spectra obtained on muscle tissue suffer from poor resolution because the magnetic susceptibility gradients caused by the heterogeneous nature of the muscle tissue result in a broadening of the proton lines (*17*). In addition, residual dipolar coupling and chemical shift anisotropy (CSA) can cause a line broadening as well. These problems can be overcome by magic angle spinning (MAS), where the contributions from magnetic susceptibility, dipolar coupling, and CSA are eliminated (*18*). However, the high spinning rates used in conventional MAS experiments, where a sample spinning rate in excess of a kilohertz or larger is employed in order to eliminate spinning sidebands from the isotropic metabolite spectrum, cause disruptions of cell structures and severe tissue damage as a result of the large centrifugal forces associated with fast MAS. This is an issue that has also been raised in connection with measurements on other tissues and cell cultures (*19*−*21*). Recently, phase-altered spinning sidebands (PASS), originally developed for solid state NMR (*22*), was modified for studies of biological objects (*23*). This technique separates the spinning sidebands from the isotropic center band spectrum and can be applied at substantially lower spinning rates, as low as 40 Hz in biological samples, thus preventing structural damage in the tissue. Consequently, this technique makes it possible to study postmortem processes in intact muscles with high-resolution ^{1}H NMR.

The aim of the present study was to follow dynamic changes in metabolites and water characteristics in postmortem rabbit muscle samples of different glycogen status by performing simultaneous ^{1}H PASS NMR metabolite spectroscopy, single pulse ^{31}P NMR metabolite spectroscopy, and ^{1}H water T_2 relaxometry. The present study demonstrates that introduction of slow spinning MAS NMR makes it possible for the first time to obtain simultaneous data on postmortem metabolites, pH, and water properties within a muscle sample without disruption of sample integrity. The obtained results are discussed in relation to existing results obtained using the spectroscopic techniques individually on muscle tissue.

EXPERIMENTAL PROCEDURES

Animals and Sampling. Six New Zealand White female rabbits weighing 3.4−3.7 kg were included in the present study. The study was performed over a 3 week period, and within this period, the animals were kept in the Animal Resource Center Facility of Pacific Northwest National Laboratory. Before the experiments were started, the animals were randomized by weight and divided into two groups: a control group ($n = 3$) and a group that was treated with adrenaline to reduce muscle glycogen stores ($n = 3$). Adrenaline treatment consisted of subcutaneous injection (0.5 mg/kilo body weight) 4 h before sacrifice. Both groups of animals were withdrawn from feed 4 h before sacrifice. All animals were sacrificed by exposure to 100% CO_2 gas for 4 min (2 min after respiration stopped). *M. psoas major* was immediately excised, and a muscle sample (approximately 300 mg) was cut out and carefully inserted from the bottom into an open 7.5 mm O.D. (6 mm I.D.) rotor used for the NMR experiments (see below) whereafter two Teflon plucks were inserted into the rotor. Because one Teflon plug has a whole ($\sim\phi$ 0.1 mm) at the middle for the air to escape, essentially approaching zero pressure was applied to the muscle sample during the sample loading process. Acquisition of NMR data was started between 12 and 15 min postmortem. The remaining part of the *M. psoas major* was wrapped in polyethylene film and stored at 25 °C for 4 h and subsequently at 4 °C until the determination of WHC (see below).

NMR Experiments. All experiments were performed on a Chemagnetics 300 MHz Infinity Spectrometer, with a proton Larmor frequency of 299.982 MHz. A standard CP/MAS probe with a 7.5 mm O.D. and a 6 mm I.D. pencil type spinner system equipped with a flat drive tip and an airflow restriction in the driver channel was used. The rotor was marked with three equally spaced precision marks for optical detection of the spinning rate. A sample spinning rate of 40 Hz was used, and a standard Chemagnetics MAS speed controller was used to regulate the spinning rate with an accuracy of approximately ±0.3 Hz. Hence, the maximum centrifugal force in the periphery of the sample is 19*g* and rapidly decreases to 0*g* in the center of the rotor. We found no observable macroscopic changes in the muscle sample after spinning at this speed.

A protocol containing three different measurements was established as follows: (i) the ^{1}H two-dimensional (2D) PASS experiment to measure (water-suppressed) metabolite spectrum, (ii) the single pulse ^{31}P experiment to determine the ^{31}P metabolite spectrum, and (iii) the ^{1}H Carr−Purcell−Meiboom−Gill (CPMG) experiment to determine the water T_2 relaxation. The ^{1}H 2D PASS experiment was performed as described previously (*23*). The $\pi/2$ pulse width was 16 μs, and water suppression was achieved by implementing the DANTE pulse sequence prior to the start of the ^{1}H 2D PASS segment. The DANTE pulse sequence consisted of 4000 pulses with a tip angle of about 5° and equally spaced by 100 μs. The ^{1}H 2D PASS sequence with 16 evolution steps was used for the measurement. For each of the 16 evolution steps, a total of eight scans were acquired with a recycle delay of 1 s, resulting in a total acquisition time of 4 min. Each ^{31}P spectrum was acquired using an average of 64 scans with a recycle delay of 3 s, resulting in a total acquisition time of 3.5 min. The acquisition parameters used were 1024 points per FID and a spectral width of 20 kHz. The ^{1}H CPMG experiment was performed with a time between subsequent 180° pulses of 250 μs, and the 90 and 180° pulse times were 16 and 32 μs, respectively. The amplitude of each echo in a train of 1024 echoes was acquired as a single FID with a recycle delay of 4 s and an accumulation number of 32. The total acquisition time for each CPMG experiment was 3.0 min. All NMR experiments were carried out at a temperature of 15 °C.

Supplementary Total Correlation Spectroscopy (TOCSY) NMR Experiments. A ^{1}H−^{1}H 2D TOCSY (*27*) experiment was measured on a rabbit muscle sample after 24 h postmortem, and the resulting 2D spectrum was used to assist in assigning the proton metabolite lines. The TOCSY experiments were performed with a sample spinning rate of 3 kHz. Hence, in this way, the PASS sequence was not needed, resulting in a much shorter measuring time than in an experiment where PASS was extended with a TOCSY sequence. As mentioned above, the disadvantage of this method is that the tissue structure is damaged and a large fraction of the water is driven out of the tissue. Hence, the assignments of the TOCSY spectra must be done with care, as the lines might have shifted due to the structural alterations in the sample. The TOCSY spectra were acquired at 15 °C with the Hyper Complex TOCSY sequence. The spectral widths of both dimensions were 3 kHz, corresponding to a dwell time of 333.33 μs. A total of 512 increments of 32 transients per increment were collected with 2k data points along the acquisition dimension (e.g., with a acquisition time of 0.683 s), and a spin lock time of 70 ms was used. This corresponds to a maximum evolution time of 170 ms. The recycle delay time was 1 s. Water suppression was achieved using DANTE using 4000 small tip angle pulses (∼5°) spaced by 100 μs prior to the start of TOCSY sequence (water suppression is necessary due to the limited dynamic range of the spectrometer). The resulting total experimental time was about 10 h.

Postprocessing of NMR Data. The ^{1}H 2D PASS spectrum was obtained after 2D Fourier transformation of the 2D PASS data with 16 points along the evolution dimension. For the ^{31}P spectra, chemical shifts and integrals of signals were calculated using the spectrometer build-in functions. The ^{1}H spectra chemical shifts are reported in ppm

relative to tetramethylsilane via internally referencing to the methyl line of creatine at 3.03 ppm, and in the ^{31}P spectra, chemical shifts are reported in ppm relative to the PCr resonance at 0.0 ppm. In the ^{31}P spectra, the amounts of various metabolites are expressed as relative signal intensities assuming a total amount of phosphor metabolites in the muscle tissue of 50 μmol/g (*14*).

From the obtained ^{1}H 2D PASS spectra and ^{31}P spectra, the pH of the muscle tissue was calculated from the chemical shift of the histidine C-6 proton and inorganic phosphate, respectively, using eqs 1 and 2:

$$\mathrm{pH}_{C-2} = \mathrm{p}K_a + \log\left(\frac{\delta_A - \delta}{\delta - \delta_B}\right) \quad (1)$$

$$\mathrm{pH}_{\pi} = \mathrm{p}K_a + \log\left(\frac{\delta_A - \delta}{\delta - \delta_B}\right) \quad (2)$$

where pK_a is the acid dissociation constant, δ_A and δ_B are the chemical shifts of the acid and alkaline, respectively, and δ is the observed chemical shift. For C-6 histidine, pK_a was set to 7.14, δ_A and δ_B were set to 8.58 and 7.66, respectively, as reported by Damon et al. (*28*). For inorganic phosphate, pK_a was set to 6.82, and δ_A and δ_B were set to 3.24 and 5.67, respectively (*28*).

The ^{1}H CPMG data were analyzed using distributed exponential fitting analysis using the RI Win-DXP program (software release 1.2.3) released from Resonance Instruments Ltd., U.K. A continuous distribution of exponentials for a CPMG experiment may be defined by eq 3:

$$g_i = \int_0^{\infty} A(T) \times e^{-ti/T}\,\mathrm{d}T \quad (3)$$

where g_i is the intensity of the decay at time *ti*, and $A(T)$ is the amplitude of the component with transverse relaxation time T. The RI Win-DXP program solves this equation by minimizing the function 4:

$$(g_i - \int_{x=1}^{m} f_x e^{-\tau i/Tx})^2 + \lambda \sum_{x=1}^{m} {}^m f_x^2 \quad (4)$$

where $f_x = \int_{T_x}^{T_{x+1}} A(T)\,\mathrm{d}T$. $\lambda \sum_{x=1} {}^m f_x^2$ is a linear combination of functions added to the equation in order to perform a zero-order regularization as described by Press et al. (*29*). The data were pruned from 1024 to 256 points using linear pruning, which on synthetic data was found to give robust solutions. This analysis resulted in a plot of relaxation amplitude for individual relaxation processes vs relaxation time. From such analyses, the time constant for each peak was calculated from the peak position, and the corresponding water fractions were determined by cumulative integration. All calculations were carried out using an in-house program written in Matlab (The Mathworks Inc., Natick, MA).

Determination of WHC. WHC was determined by centrifugation of samples at 21 h postmortem using the following procedure. From each animal, four subsamples, approximately 1 cm long and having a cross-sectional area of approximately 3 mm × 3 mm (weight approximately 0.3−0.5 g), were cut out parallel to the fiber direction from *M. psoas major*. The subsamples were weighed and placed in tubes (Mobicols from MoBiTec, Göttingen, Germany) with a filter (pore size 90 μm) in the bottom of the tubes to separate the meat from the expelled liquid. The samples were then centrifuged at 100*g* for 30 min at a temperature of 20 °C. After centrifugation, the samples were weighed again, and the centrifugation loss was calculated as the percentage difference in weight before and after centrifugation.

Statistical Analysis. Statistical analyses were carried out with the Statistical Analysis System (SAS Institute Inc., Cary, NC). Regression analysis (Proc REG) was used for comparison of pH determinations, and analysis of variance (Proc MIXED) was used for testing the effects of treatment and measurement time on the measured variables. The statistical model included the fixed effects of measurement time and treatment (adrenaline vs control) and the random effect of animal within treatment.

RESULTS

^{31}P Data. Typical ^{31}P spectra recorded on a muscle sample with low and normal glycogen content at 15 min postmortem

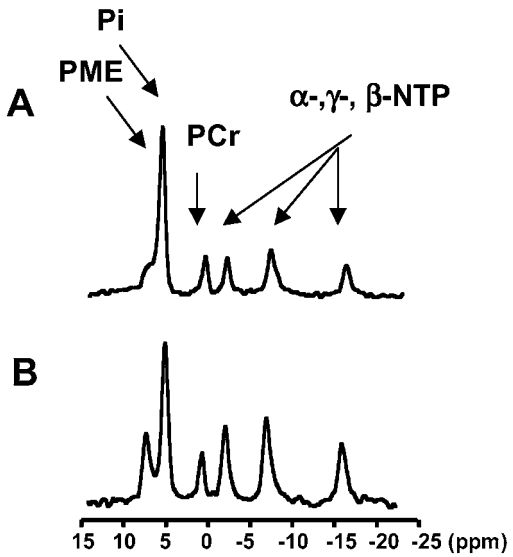

Figure 1. ^{31}P spectra recorded on a sample from an adrenaline-treated animal (**A**) and on a sample from a control animal 15 min postmortem (**B**).

Table 1. Results from Analysis of Phosphorus Data[a]

	control ($n = 3$)	adrenaline ($n = 3$)	significance level
K_{PCr} (μmol/g)	5.65 (1.57)	2.36 (1.57)	$p = 0.21$
half-life PCr (min)	28.1 (4.4)	26.1 (4.4)	$p = 0.80$
NTP initial level (μmol/g)	5.8 (0.2)	3.9 (0.2)	$p = 0.01$**
NTP degradation rate (mmol/g/min^{-1})	58.9 (8.3)	58.0 (8.3)	$p = 0.95$

[a] LS means, standard error (SE), and level of significance within rows are shown.

are shown in **Figure 1**. Resonances from phosphomonoesters (~7 ppm), inorganic phosphate (π) (~5 ppm), PCr (0 ppm), and γ-, α-, and β-phosphate groups in NTP (~ −6.5, −11, and −20 ppm) are observed. During the measuring period, a decrease in the PCr concentration and subsequently a deprivation of NTP were seen. In agreement with previous observations (*14*−*15*, *30*) the postmortem decrease in [PCr] was found to be exponential and accordingly described by the following eq 5:

$$[\mathrm{PCr}] = K_{\mathrm{PCr}} \exp(-b_{\mathrm{PCr}}\mathrm{time}) \quad (5)$$

where K_{PCr} and b_{PCr} are coefficients. The rate of PCr breakdown and the half-life of PCr (ln $2/b_{PCr}$) are given in **Table 1**. The degradation of NTP was found to decline linearly, and accordingly, data were fitted to a linear function, where the slope expressed the rate of degradation, and the intersection expressed the initial level. **Table 1** summarizes the phosphorus data. The biological variation between the animals is clearly depicted in the standard errors. A tendency for higher initial levels of PCr (K_{PCr}) and higher half-life was observed for control samples; however, the differences were not significant. In contrast, the initial level of NTP was found to be significantly higher in control samples than in samples from adrenaline-treated animals, whereas the rate of NTP degradation was found to be similar for the two groups. **Figure 2** displays the postmortem changes in pH as calculated from the chemical shifts of π. A dramatic effect of adrenaline treatment on the pH development was seen, as it both significantly increased the pH measured 13 min postmortem and reduced the extent of pH decrease postmortem.

^{1}H PASS. Figure 3A shows a typical ^{1}H spectrum obtained on a static muscle sample, and **Figure 3B** shows the centerband

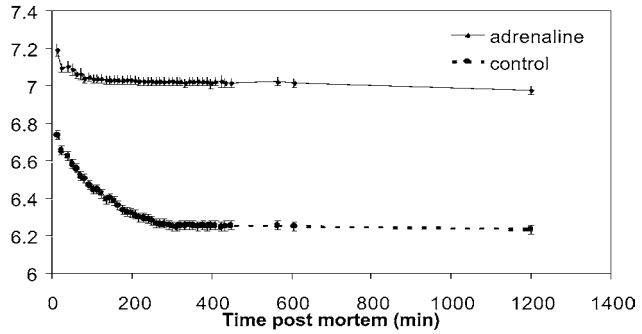

Figure 2. Development in pH as calculated from the chemical shift of π. Least squares means for muscle samples from adrenaline ($n = 3$) and control animals ($n = 3$) are given. Bars show standard errors.

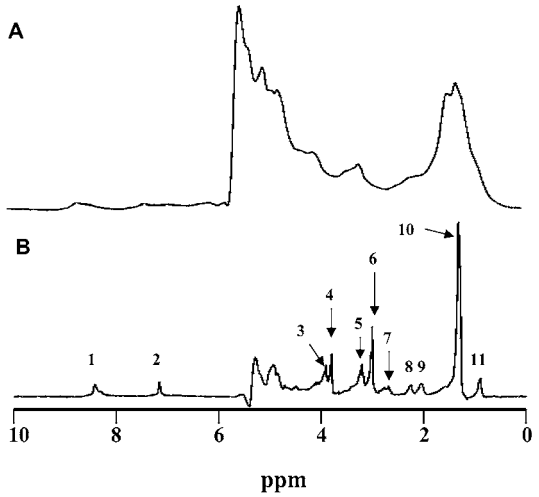

Figure 3. Examples of water-suppressed ^{1}H NMR metabolite spectrum of a control muscle sample 24 h postmortem obtained on a static sample (**A**) and with 40 Hz MAS using the PASS technique (**B**). The main resonances observed in **Figure 5B** are assigned as follows: 1 (~8.5 ppm), histidine 6-CH; 2 (7.2 ppm), histidine 8-CH; 3 (3.9 ppm), creatine methylene; 4 (~3.8 ppm), 2-CH of amino groups; 5 (3.2 ppm), choline/pcho methyl; 6 (3.0 ppm), creatine methyl; 7 (~2.7 ppm), lipid (=CH–**CH$_2$**–CH=); 8 (2.2 ppm), lipid (–OOC–**CH$_2$**–); 9, (2.0 ppm), lipid (CH$_2$–**CH$_2$**–CH=); 10 (~1.3 ppm), lactate methyl and lipid $(CH_2)_n$; and 11, lipid methyl.

of ^{1}H 2D PASS spectrum obtained on a muscle sample at a sample spinning rate of 40 Hz. A tremendous improvement in resolution is obtained using the PASS technique, allowing detection of several metabolites in the muscle tissue. In part based on the results of the TOCSY experiment (**Figure 4**), the resonances are tentatively identified and given in the figure caption. No major changes neither between control and adrenaline-treated animals nor between measuring postmortem times were observed in the ^{1}H PASS spectra in the chemical shift region 0−5 ppm. In contrast, noticeable changes were observed in the 6.5−9 ppm region; see **Figure 5**. Two histidine peaks were observed in the 8.3−8.6 ppm region, and these peaks had different chemical shift in the control and the adrenaline-treated animals, which can be explained by a difference in pH between the two types of samples. Finally, in the control sample, a new peak at 6.8 ppm appeared during the postmortem period.

pH was calculated from the chemical shift of histidine C-6 protons (using the dominant downfield peak when splitting occurred), and the ability of the two pH measurements by the chemical shifts of π and histidine C-6 to produce equivalent results was tested by comparing the obtained values as shown in **Figure 6**. Regression of the pH values from the π data on the pH values from C-6 data yielded an intercept that was not statistically different from zero (-0.40 ± 0.07) and a slope that was not statistically different from one (1.08 ± 0.01).

Water ^{1}H T_2 Data. Figure 7 displays typical examples of CPMG data obtained 30 min and 20 h postmortem after distributed exponential fitting. Three components, hereafter referred to as T_{2A}, T_{2B}, and T_{2C}, were detected in all muscle samples: a minor component with a relaxation time between 1 and 10 ms (T_{2A}), a major component with a relaxation time between 30 and 50 ms (T_{2B}), and finally a third component with a relaxation time between 150 and 500 ms (T_{2C}). During the postmortem period, a dramatic increase in the T_{2C} population was observed (**Figure 8A**). The observed increase was significantly reduced by adrenaline treatment with a much more pronounced increase in the control samples as compared with samples from adrenaline administered animals. In addition, the T_{2B} time constant was significantly lower in samples from adrenaline-treated animals than in the controls (**Figure 8B**).

WHC. Centrifugation of muscle samples at 21 h postmortem revealed significant differences ($p = 0.07$) in WHC between muscle samples from control and adrenaline-treated animals with mean values of 1.9 and 0.9% weight loss, respectively.

DISCUSSION

High-resolution MAS NMR has proven useful for analysis of intact tissues, and high-quality spectra have been demonstrated on various tissues (*27*, *31*−*35*). Moreover, it has been shown that the recently developed PASS method makes it possible to obtain high-resolution ^{1}H NMR metabolite spectra in intact muscle tissue at very low spinning rates (*23*), thus eliminating damage to sample structure. MAS at a spinning speed of just 40 Hz was in the present study shown to result in well-resolved spectra of muscle tissue, where several lines could be detected and assigned to various metabolites (**Figure 3**). Interestingly, the ^{1}H PASS spectra revealed the appearance of a new peak at 6.8 ppm during the postmortem period in the control samples. Contrary, this peak did not appear in samples from adrenaline-treated animals (**Figure 5**). The 6.8 ppm peak has only rarely been reported in previous ^{1}H NMR spectroscopic studies on muscles (*36*). However, the 6.8 ppm peak was recently reported occasionally to appear during exercise of muscles (*28*). The peak was suggested to reflect a splitting of the already existing 7.2 ppm histidine C-8 proton peak, and the presence of the two resonances was suggested to reflect the presence of histidine in oxidative and glycolytic muscle fibers, respectively, having different pH values (*28*). The rabbit *psoas* muscle used in the present study is known to be composed almost entirely of glycolytic fibers (*37*). However, the 6.8 ppm peak also emerged in this muscle, which is in disagreement with the ascription of the resonance to histidine C-4 protons in a different pH environment than the 7.2 ppm peak. Moreover, if the 7.2 and 6.8 ppm peaks represent identical histidine C-4 proton groups in different compartments, the observed splitting would correspond to an unrealistic high pH gradient within a muscle. Arus et al. (*36*) have ascribed the 6.8 ppm peak to the aminoprotons in creatine. The absence of the peak initially postmortem and in adrenaline-treated muscles reveals that its appearance is pH dependent. This may be explained by a pH effect on the exchange rate between the amino protons and the water protons and thereby the NMR visibility of these protons. This would explain the rare observations of the peak (*36*) and also the fact that it appeared during exercise of muscles (*28*), where a pH decrease is taking place due to lactate accumulation. Finally, the 6.8 ppm peak may originate from tyrosine, as two

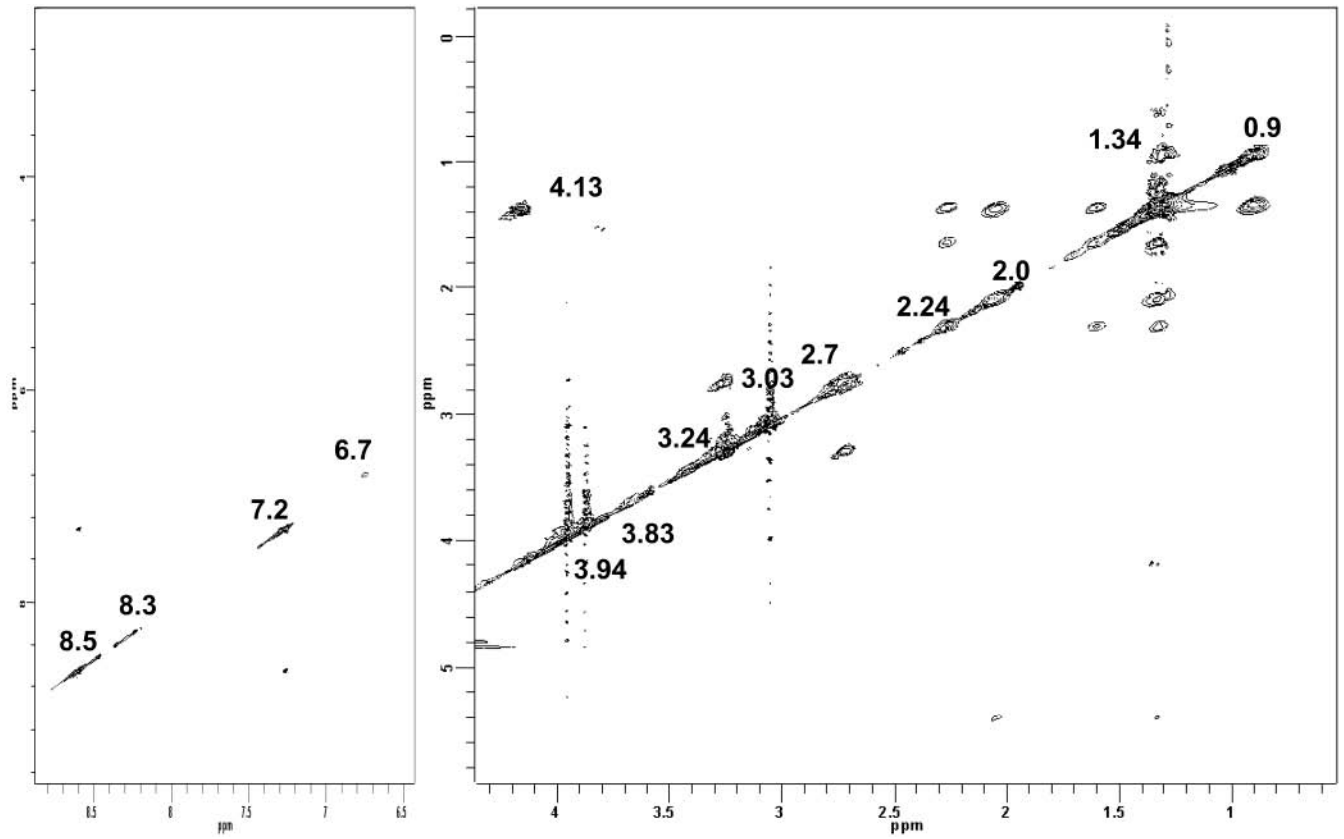

Figure 4. Water-suppressed ^{1}H–^{1}H TOCSY MAS NMR spectrum of the muscle from the control animal as **Figure 5**.

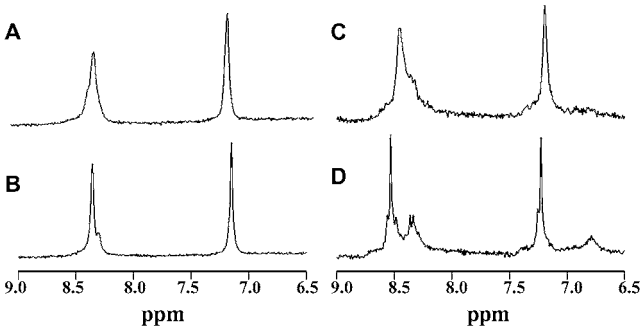

Figure 5. Typical examples of ^{1}H PASS spectra in the 6.5–9 ppm region acquired on a muscle sample from adrenaline-treated animals at 20 min postmortem (**A**), on a muscle sample from adrenaline-treated animals at 20 h postmortem (**B**), on a muscle sample from control animals at 20 min postmortem (**C**), and on a muscle sample from control animals at 20 h postmortem (**D**).

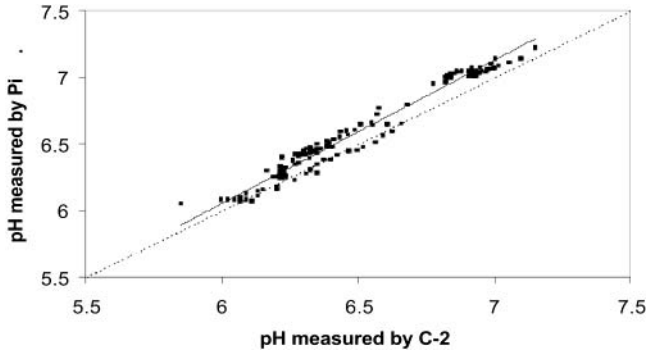

Figure 6. Regression analysis of ^{31}P and ^{1}H methods for measuring pH. The solid line indicates the best least squares fit of the data, and the dashed line indicates unity.

of the aromatic protons have a chemical shift in this range (*38*). Tyrosine is present in the muscle proteins but is most probably NMR invisible as the tyrosine residues are located in the hydrophobic interior of native proteins. The postmortem pH decrease triggers protein denaturation, which is known to result in exposure of hydrophopic amino acid residues to the exterior environment (*39*−*41*). Exposure of hydrophobic amino acid residues may become NMR visible. Consequently, the present data might reflect that protein denaturation occurred in muscles from control animals but not in muscles from adrenaline-treated animals where the pH decrease was almost eliminated. This is in agreement with expectations of the outcome of a postmortem pH decrease on muscle proteins (*42*). Previous studies have only dealt with the investigation of the effect of pH on muscle proteins only indirectly by studying the solubility of extracted proteins (*43*−*44*). In contrast, the data in the present study together with data from a recent Raman spectroscopic study on postmortem pig muscle (*45*) are extremely interesting as they both may provide direct evidence of protein denaturation from measurements on the intact, untreated muscle tissue. Further studies should be accomplished to examine the potential use of the tyrosine resonance as an indicator of protein denaturation, and NMR studies are already under progress in our lab. Elucidation of the origin of the 6.8 ppm resonance is also of relevance for the use of NMR as a tool in medical areas, where it also could be expected to have potential as an indicator in diagnosis of muscle disorders.

The combination of simultaneous ^{1}H PASS and ^{31}P NMR spectroscopy on muscle samples allowed comparison of pH determined from the chemical shift of histidine C-6 and inorganic phosphate, respectively, on a very large number of observations. In agreement with previous comparisons of the two methods (*28*, *46*−*47*), excellent correlation was found between the two methods, implying that inorganic phosphate

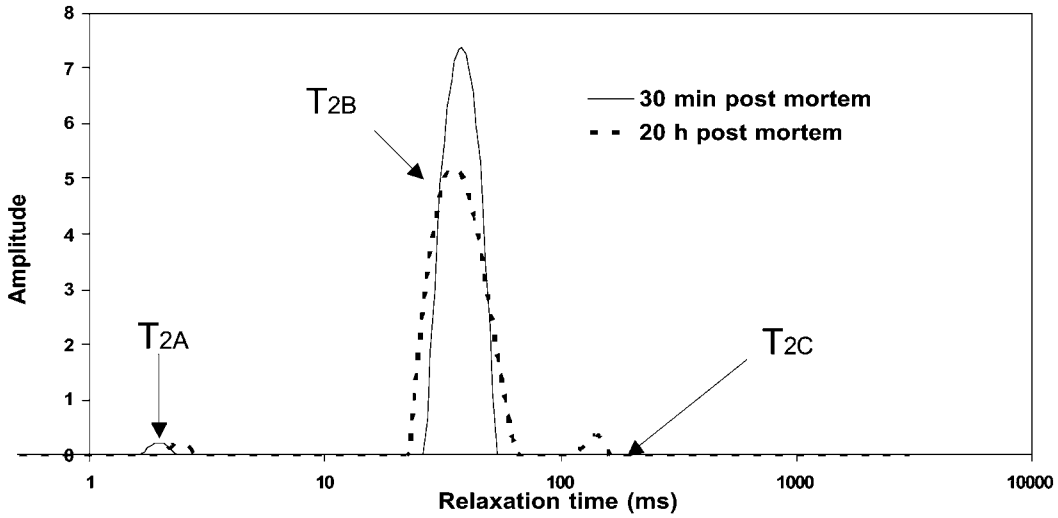

Figure 7. Distribution of the water T_2 relaxation times in a control muscle sample measured 30 min and 20 h postmortem.

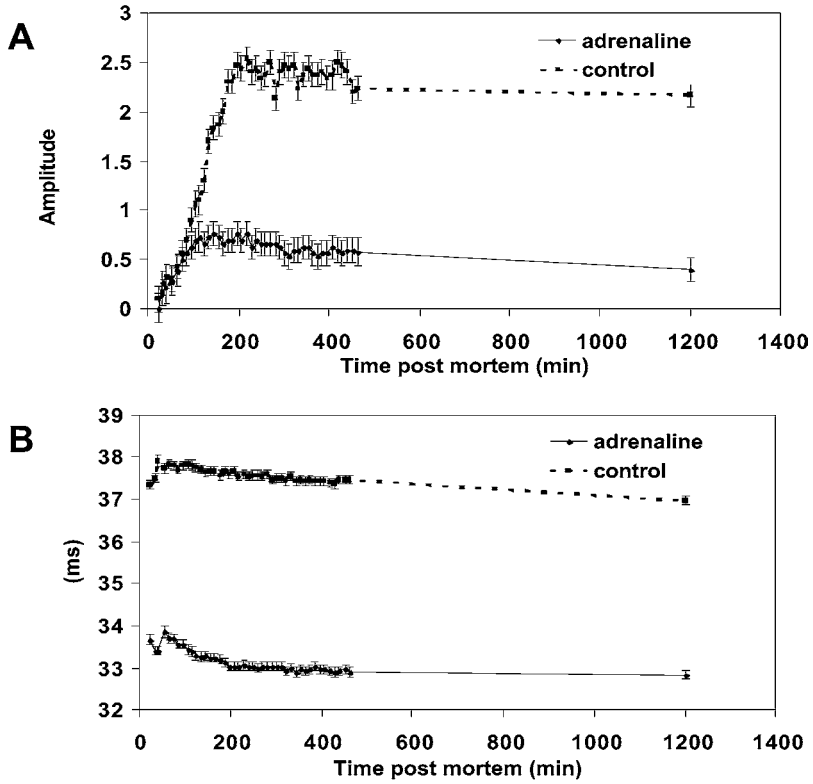

Figure 8. Postmortem course of the relative population of the T_{2C} component (**A**) and the T_{2B} time constant (**B**) in muscle samples from control (n = 3) and adrenaline-treated (n = 3) animals. Least squares means are given. Bars indicate standard errors.

and histidine share identical pH environments and that both methods are robust for pH determination in postmortem muscles.

Lactate is known to be formed and accumulated in muscles postmortem. However, an attempt to use the intensity of the 1.3 ppm peak to quantify lactate failed in the present study. This is most probably due to the fact that a high proportion (~85%) of lactate has a transverse relaxation time of about ~25 ms (*48*), which means that this lactate relaxes too fast to be detected with a spinning rate of 40 Hz. Consequently, even though the low spinning rate is associated with advantages due to the maintenance of sample integrity, it restricts the detection of certain metabolites, and further studies should be accomplished to optimize the spinning rate without compromising the advantage of slow spinning.

It is generally believed that the WHC of meat is determined by the biochemical and physical processes taking place postmortem (*1*). On the basis of microscopic studies, the occurrence of a postmortem expulsion of water from the muscle cells and formation of extramyofibrillar water channels was hypothesized as the key event (*49*). This was recently confirmed by low-field NMR transverse relaxation studies, where a redistribution of water was found to take place during the conversion of muscle to meat with an increase in the water population characterized by a transverse relaxation time (T_{2C}) of 100−300 ms (*8*). The present study supports these findings. This population with a relaxation time of 100−300 ms has previously been identified as the extramyofibrillar water and determines the amount of potential drip loss (*7*). In muscle samples from adrenaline-treated animals, only a minor increase in the T_{2C} population was observed and subsequently low centrifugation loss was found in these samples, implying that the reduced increase in the T_{2C} population T_{2C} is associated with an increased WHC.

The T_{2B} time constant, representing the myofibrillar water (*50*), has been shown to be highly affected by structural attributes of the muscle filaments. In a study where meat structure was manipulated by prerigor contraction and stretching, the T_{2B} time constant was found to be negatively correlated with the degree of contraction, which was ascribed to the spatial constrictions associated with the higher degree of overlap between the I- and the A-band (*51*). Accordingly, the lower T_{2B} time constant in samples from adrenaline-treated animals suggests a higher degree of contraction in these muscles. In this context, it is worth noticing that the ^{31}P NMR data showed significantly lower levels of ATP in muscles from the adrenaline-treated animals than in the control animals (**Table 1**). This suggests that contraction sets in earlier in these muscles. Further work should be pursued to verify a potential different contraction mechanism in glycogen-depleted muscles.

The postmortem pH decrease is known to affect the WHC of meat (*52*), which has been explained in terms of effects on protein denaturation (*42*). In addition, pH has been proven to affect the myofilament lattice spacing (*53*), and through its action on the electrostatic repulsion between myofilamentous proteins, the pH has been hypothesized to affect the amount of water located within these spaces and accordingly also the ability of the meat to retain water (*54*). However, this is the first time that direct physical evidence of the impact of the pH on the expulsion of water from muscles postmortem has been obtained. The use of preslaughter adrenaline administration in the present study succeeded in almost entirely eliminating the postmortem pH decrease (**Figure 4**), and accordingly, the sample material was optimal for investigating and comparing postmortem changes in water distribution in muscles with and without a postmortem pH decrease. Noticeably, data showed that the postmortem increase in the T_{2C} population, representing extramyofibrillar water and potential drip loss, was almost eliminated in samples from adrenaline-treated animals, implying that absence of a postmortem pH decrease eliminates the expulsion of water from myofibrillar structures into the extramyofibrillar spaces and hereby optimizes WHC. Accordingly, the present data physically demonstrate that indeed the pH is a key factor in controlling the expulsion of water from myofibrillar structures.

In conclusion, in the present study, ^{1}H PASS NMR metabolite spectroscopy, ^{31}P NMR metabolite spectroscopy, and ^{1}H CPMG water measurements have been combined on the same muscle tissue for the first time to study the postmortem processes in rabbit muscles. The use of preslaughter adrenaline administration almost eliminated the postmortem pH decrease in muscles, and the measurement of the muscle T_2 distribution revealed that pH is controlling the extent of postmortem expulsion of water from myofibrillar structures, which was also reflected in the WHC of the tissue. ^{31}P and ^{1}H PASS NMR spectroscopy have been used to follow changes in the pH and the metabolite composition as a function of the postmortem time. Interestingly, the ^{1}H spectrum revealed the appearance of a new resonance at 6.8 ppm during the postmortem period, which was absent in muscles from adrenaline-treated animals. The emerging peak may reflect NMR visibility of tyrosine upon denaturation of proteins, but further studies are needed to confirm this hypothesis.

ACKNOWLEDGMENT

The research was performed in the Environmental Molecular Sciences Laboratory (a national scientific user facility sponsored by the DOE Biological and Environmental) located at the Pacific Northwest National Laboratory and operated for DOE by Battelle.

LITERATURE CITED

(1) Offer, G.; Knight, P. The structural basis of water-holding in meat Part 2: Drip Losses. In *Developments in Meat Science 4*; Lawrie, R., Ed.; Elsevier Applied Science: London, 1988; Chapter 4, pp 172−243.

(2) Lambert, I. H.; Nielsen, J. H.; Andersen, H. J.; Ørtenblad, N. Cellular model for induction of drip loss in meat. *J. Agric. Food Chem.* **2001**, *49*, 4876−4883.

(3) Tornberg, E.; Andersson, A.; Göransson, Å.; von Seth, G. Water and Fat Distribution in Pork in Relation to Sensory Properties. In *Pork Quality: Genetic and Metabolic Factors*; Puolanne, E., Demeyer, D. I., Ruusunen, M., Ellis, S., Eds.; CAB International: Wallingford, United Kingdom, 1993.

(4) Brown, R. J. S.; Capozzi, F.; Cavani, C.; Cremonini, M. A.; Petracci, M.; Placucci, G. Relationships between ^{1}H NMR Relaxation Data and Some Technological Parameters of Meat: A Chemometric Approach. *J. Magn. Reson.* **2000**, *147*, 89−94.

(5) Brøndum, J.; Munck, L.; Henckel, P.; Karlsson, A.; Tornberg, E.; Engelsen, S. B. Prediction of Water-holding Capacity and Composition of Porcine Meat with Comparative Spectroscopy. *Meat Sci.* **2000**, *55*, 177−185.

(6) Bertram, H. C.; Andersen, H. J.; Karlsson, A. H. Comparative study of low-field NMR relaxation measurements and two traditional methods in the determination of water holding capacity of pork. *Meat Sci.* **2001**, *57*, 125−132.

(7) Bertram, H. C.; Dønstrup, S.; Karlsson, A. H.; Andersen, H. J. Continuous distribution analysis of T_2 relaxation in meat—an approach in the determination of water holding capacity. *Meat Sci.* **2002**, *60*, 279−285.

(8) Bertram, H. C.; Karlsson, A. H.; Andersen, H. J. The significance of cooling rate on water dynamics in porcine muscle from heterozygote carriers and noncarriers of the halothane gene -A low-field NMR relaxation study. *Meat Sci.* **2004**, *65*, 1281−1291.

(9) Hoult, D. I.; Busby, S. J. W.; Gadian, D. G.; Radda, G. K.; Richards, R. E.; Seeley, P. J. Observation of tissue metabolites using ^{31}P nuclear magnetic resonance. *Nature (London)* **1974**, *252*, 285−287.

(10) Burt, C. T.; Glonek, T.; Barany, M. Analysis of phosphate metabolites, the intracellular pH, and the state of adenosine triphosphate in intact muscle by phosphorous nuclear magnetic resonance. *J. Biol. Chem.* **1976**, *251*, 2584−2591.

(11) Seeley, P. J.; Busby, S. J. W.; Gadian, D. G.; Radda, G. K.; Richards, R. E. A new approach to metabolite compartmentation in muscle. *Biochem. Soc. Trans.* **1976**, *4*, 62−64.

(12) Busby, S. J. W.; Gadian, D. G.; Radda, G.; Richards, R. E.; Seeley, P. J. Phosphorus nuclear-magnetic resonance studies of compartmentation in muscle. *Biochem. J.* **1978**, *170*, 103−114.

(13) Vogel, H. J.; Lundberg, P.; Fabiansson, S.; Ruderus, H.; Tornberg, E. Post-mortem energy metabolism in bovine muscles studied by noninvasive phosphorus-31 nuclear magnetic resonance. *Meat Sci.* **1985**, *13*, 1−18.

(14) Renou, J.-P.; Canoni, P.; Gatelier, P.; Valin, C.; Cozzone, P. J. Phosphorus-31 nuclear magnetic resonance study of *post mortem* catabolism and intracellular pH in intact excised rabbit muscle. *Biochemie* **1986**, *68*, 543−554.

(15) Bertram, H. C.; Dønstrup, S.; Karlsson, A. H.; Andersen, H. J.; Stødkilde-Jørgensen, H. *Post mortem* energy metabolism and pH development in porcine *M. longissimus dorsi* as affected by two different cooling regimes. A ^{31}P NMR spectroscopic study. *Magn. Reson. Imaging* **2001**, *19*, 993−1000.

(16) Lundberg, P.; Vogel, H. J.; Ruderus, H. Carbon-13 and proton NMR studies of post-mortem metabolism in bovine muscles. *Meat Sci.* **1986**, *18*, 133−160.

(17) Weybright, P.; Millis, K.; Campbell, N.; Cory, D. G.; Singer, S. Gradient high-resolution, magic angle spinning ^{1}H nuclear magnetic resonance spectroscopy of intact cells. *Magn. Reson. Med.* **1988**, *39*, 337−345.

(18) Andrew, E. R.; Eades, R. G. Removal of dipolar broadening of NMR spectra of solids by specimen rotation. *Nature* **1959**, *183*, 1820.

(19) Cheng, L. L.; Ma, M. J.; Becerra, L.; Hale, T.; Tracey, I.; Lackner, A.; Gonzalez, R. G. Quantitative neuropathology by high-resolution magic angle spinning proton magnetic resonance spectroscopy. *Proc. Natl. Acad. Sci. U.S.A.* **1997**, *94*, 6408−6413.

(20) Weybright, P.; Millis, K.; Campbell, N.; Cory, D. G.; Singer, S. High-resolution magic angle spinning ^{1}H nuclear magnetic resonance spectroscopy of intact cells. *Magn. Reson. Med.* **1988**, *39*, 337−344.

(21) Griffin, J. L.; Bollard, M.; Nicholson, J.; Bhakoo, K. Spectral profiles of cultured neuronal and glial cells derived from HRMAS ^{1}H NMR spectroscopy. *NMR Biomed.* **2002**, *15*, 375−384.

(22) Antzutkin, O. N.; Shekar, S. C.; Levitt, M. H. Two-dimensional sideband separation in magic-angle spinning NMR. *J. Magn. Reson.* **1995**, *A115*, 7−19.

(23) Wind, R. A.; Hu, J. Z.; Rommereim, D. N. High-resolution ^{1}H NMR Spectroscopy in Organs and Tissues Using Slow Magic Angle Spinning. *Magn. Reson. Med.* **2001**, *46*, 213−218.

(24) Fernandez, X.; Forslid, A.; Maagaard, M.; Moeller, B. M.; Tornberg, E. Effect of time between adrenaline injection and slaughter on the rate and extent of post-mortem metabolism in porcine skeletal muscle. *Meat Sci.* **1992**, *31*, 287−298.

(25) Henckel, P.; Karlsson, A.; Oksbjerg, N.; Petersen, J. S. Control of post mortem pH decrease in pig muscles: experimental design and testing of animal models. *Meat Sci.* **2000**, *55*, 131−138.

(26) Bendall, J. R.; Lawrie, R. A. The effect of pretreatment with various drugs on post-mortem glycolysis and the onset of rigor mortis in rabbit skeletal muscle. *J. Comp. Pathol.* **1962**, *72*, 118−130.

(27) Garrod, S.; Humpfer, E.; Spraul, M.; Connor, S. C.; Polley, S.; Connelly, J.; Lindon, J. C.; Nicholson, J. K.; Holmes, E. High-resolution magic angle spinning ^{1}H NMR spectroscopic studies on intact rat renal cortex and medulla. *Magn. Reson. Med.* **1999**, *41*, 1108−1118.

(28) Damon, B. M.; Hsu, A. C.; Stark, H. J.; Dawson, M. J. The carnosine C-2 proton's chemical shift reports intracellular pH in oxidative and glycolytic muscle fibers. *Magn. Reson. Med.* **2003**, *49*, 233−240.

(29) Press, W. H.; Teukolsky, S. A.; Vetterling, W. T.; Flannery, B. P. Integral Equations and Inverse Theory. *Numerical Recipes in Fortran*, 2nd ed.; Cambridge University Press: New York, 1992; pp 289−341.

(30) Azuma, Y.; Manabe, N.; Kawai, F.; Kanamori, M.; Miyamoto, H. Phosphorus-31 nuclear magnetic resonance study of energy metabolism in intact slow- and fast-twitch muscles of rats. *J. Anim. Sci.* **1994**, *72*, 103−108.

(31) Bollard, M. E.; Garrod, S.; Holmes, E.; Lindon, J. C.; Humpfer, E.; Spraul, M.; Nicholson, J. K. High-resolution ^{1}H and ^{1}H-^{13}C magic angle spinning NMR spectroscopy of rat liver. *Magn. Reson. Med.* **2000**, *44*, 201−207.

(32) Swanson, M. G.; Vigneron, D. B.; Tabatabai, Z. L.; Males, R. G.; Schmitt, L.; Carroll, P. R.; James, J. K.; Hurd, R. E.; Kurbanewicz, J. Proton HR_MAS spectroscopy and quantitative pathologic analysis of MRI/3D-MRSI-targeted postsurgical prostate tissues. *Magn. Reson. Med.* **2003**, *50*, 944−954.

(33) Wu, C.-L.; Taylor, J. L.; He, W.; Zepeda, A. G.; Halpern, E. F.; Bielecki, A.; Gonzalez, R. G.; Cheng, L. L. Proton high-resolution magic angle spinning NMR analysis of fresh and previously frozen tissue of human prostate. *Magn. Reson. Med.* **2003**, *50*, 1307−1311.

(34) Rooney, O. M.; Troke, J.; Nicholson, J. K.; Griffin, J. L. High-resolution diffusion and relaxation-edited magic angle spinning ^{1}H NMR spectroscopy of intact liver tissue. *Magn. Reson. Med.* **2003**, *50*, 925−930.

(35) Taylor, J. L.; Wu, C. L.; Cory, D.; Gonzalez, R. G.; Bielecki, A.; Cheng, L. L. High-resolution magic angle spinning proton NMR analysis of human prostate tissue with slow spinning rates. *Magn. Reson. Med.* **2003**, *50*, 627−632.

(36) Arús, C.; Bárány, M.; Westler, W. M.; Markley, J. L. ^{1}H NMR of intact muscle at 11 T. *FEBS Lett.* **1984**, *165*, 231−237.

(37) Wahr, P. A.; Metzger, J. M. Peak power output is maintained in rabbit psoas and rat soleus single muscle fibers when CTP replaces ATP. *J. Appl. Physiol.* **1988**, *85*, 76−83.

(38) Sharma, U.; Atri, S.; Sharma, M. C.; Sarkar, C.; Jagannathan, N. R. Skeletal muscle metabolism in Duchenne muscular dystrophy (DMD): an in-vitro proton NMR spectroscopy study. *Magn. Reson. Imaging* **2003**, *21*, 145−153.

(39) Steinhardt, J.; Stocker, N. Remasking of hidden tyrosines of human serum albumins after exposure to high and low pH. *Biochemistry* **1973**, *12*, 2798−2802.

(40) Goto, Y.; Takahashi, N.; Fink, A. L. Mechanism of acid-induced folding of proteins. *Biochemistry* **1990**, *29*, 3480−3488.

(41) Lala, A. K.; Kaul, P. Increased exposure of hydrophobic surface in molten globule state of α-lactalbumin: fluorescence and hydrophobic photolabeling studies. *J. Biol. Chem.* **1992**, *267*, 19914−19918.

(42) Offer, G. Modeling of the formation of pale, soft and exudative meat: Effects of chilling regime and rate and extent of glycolysis. *Meat Sci.* **1991**, *30*, 157−184.

(43) Sayre, R. N.; Briskey, E. J. Protein Solubility as Influenced by Physiological Conditions in the Muscle. *J. Food Sci.* **1963**, *28*, 675−679.

(44) Warner, R. D.; Kauffman, R. G.; Greaser, M. L. Muscle Protein Changes *Post Mortem* in Relation to Pork Quality Traits. *Meat Sci.* **1997**, *45*, 339−352.

(45) Pedersen, D. K.; Morel, S.; Andersen, H. J.; Engelsen, S. B. Early prediction of water-holding capacity in meat by multivariate vibrational spectroscopy. *Meat Sci.* **2003**, *65*, 581−592.

(46) Pan, J. W.; Hamm, J. R.; Rothman, D. L.; Schulman, R. G. Intracellular pH in human skeletal muscle by ^{1}H NMR. *Proc. Natl. Acad. Sci. U.S.A.* **1988**, *85*, 7836−7839.

(47) Hitzig, B. M.; Perng, W.-C.; Burt, T.; Okunieff, P.; Johnson, D. C. ^{1}H NMR measurement of fractional dissociation of imidazole in intact animals. *Am. J. Physiol.* **1994**, *35*, 1008−1015.

(48) Jouvensal, L.; Carlier, P. G.; Bloch, G. Evidence for biexponential transverse relaxation of lactate in excised rat muscle. *Magn. Reson. Med.* **1999**, *41*, 624−626.

(49) Offer, G.; Cousins, T. The mechanism of drip production: formation of two compartments of extracellular space in muscle *post mortem*. *J. Sci. Food Agric.* **1992**, *58*, 107−116.

(50) Bertram, H. C.; Karlsson, A. H.; Rasmussen, M.; Dønstrup, S.; Petersen, O. D.; Andersen, H. J. The origin of multiexponential T_2 relaxation in muscle myowater. *J. Agric. Food. Chem.* **2001**, *49*, 3092−3100.

(51) Bertram, H. C.; Purslow, P. P.; Andersen, H. J. Relationship between meat structure, water mobility and distribution -a low-field nuclear magnetic resonance study. *J. Agric. Food Chem.* **2002**, *50*, 824−829.

(52) Bendall, J. R.; Swatland, H. J. A review of the relationships of pH with physical aspects of pork quality. *Meat Sci.* **1988**, *24*, 85−126.

(53) Rome, E. Light and X-ray diffraction studies of the filament lattice of glycerol-extracted rabbit psoas muscle. *J. Mol. Biol.* **1967**, *27*, 591−602.

(54) Hamm, R. Functional properties of the myofibrillar system and their measurements. In *Muscle as Food*; Bechtel, P. J., Ed.; Academic Press: Orlando, 1986; pp 135−199.

Received for review August 19, 2003. Revised manuscript received February 9, 2004. Accepted February 26, 2004. The Danish Veterinary and Agricultural Research Council (SJVF) is gratefully acknowledged for financial support of the project.

JF030614Y